Nuclear Materials and Energy 9 (2016) 610–615

Contents lists available at ScienceDirect

Nuclear Materials and Energy

journal homepage: www.elsevier.com/locate/nme

Effect of Cr/Al contents on the 475°C age-hardening in oxide dispersion strengthened ferritic steels

Wentuo Han[a,b,*], Kiyohiro Yabuuchi[b], Akihiko Kimura[b], Shigeharu Ukai[c], Naoko Oono[c], Takeji Kaito[d], Tadahiko Torimaru[e], Shigenari Hayashi[f]

[a] School of Materials Science and Engineering, University of Science and Technology Beijing, Beijing, 100083, China
[b] Institute of Advanced Energy, Kyoto University, Gokasho, Uji, Kyoto, 611-0011, Japan
[c] Material Science and Engineering, Faculty of Engineering, Hokkaido University, Sapporo 060-8626, Japan
[d] Advanced Nuclear System R&D Directorate, Japan Atomic Energy Agency, Oarai, Ibaraki 311-1393, Japan
[e] Nippon Nuclear Fuel Development Co. Ltd., Oarai, Ibaraki, 311-1313, Japan
[f] Department of Metallurgy and Ceramics Science, Tokyo Institute of Technology, Tokyo, 152-8550, Japan

ARTICLE INFO

Article history:
Available online 3 June 2016

Keywords:
ODS ferritic steel
475°C embrittlement
Al and Cr effects
Cr-enriched α' phase
Hardness evolution

ABSTRACT

The age-hardening in oxide dispersion strengthened (ODS) ferritic steels with various additions of Cr (12, 15 and 18 wt.%) and Al (0, 5, 7 and 9 wt.%) were investigated. After 5000 h aging at 475°C, the hardness increases in all these ODS steels, while the increased level depends on the Cr/Al contents. In 12Cr-ODS steels, the more the Al, the higher the increased hardness is. However, in 18Cr-ODS steels, higher Al addition suppresses the age-hardening. TEM observations of 18Cr-ODS steels reveal that 9Al suppresses the formation of Cr-enriched α' phase, while the 18Cr-5Al-ODS steel comprises a plenty of α' phases. Adding Zr in ODS steels appears to increase the age-hardening. The susceptibility to age-hardening is remarkably lower in the ODS ferritic steels than in the non-ODS ferritic steel with the similar concentration of Cr.

1. Introduction

Oxide dispersion strengthened (ODS) ferritic/martensitic steels, which possess high resistances to the neutron irradiation embrittlement and void swelling, as well as good performances of mechanical properties at elevated temperatures, have been considered to be promising blanket structural materials of fusion systems and cladding materials of Generation IV nuclear energy systems, such as supercritical pressurized water reactor (SCPWR), sodium-cooled fast reactor (SFR) and lead bismuth-cooled fast reactor (LFR) [1,2].

Oxide dispersion strengthened (ODS) ferritic/martensitic steels containing 9 – 12 wt.% chromium have been developed as the fuel cladding material for SFR due to their high creep strength at elevated temperatures and enough resistance to neutron irradiation embrittlement. However, the 9 – 12 wt.%Cr-ODS ferritic/martensitic steels are not suitable for SCWR owing to an insufficient corrosion resistance of the materials [1,3]. For insuring the corrosion resistance of claddings, ODS ferritic steels with a higher Cr concentration and Al addition are highly required. However, with a Cr content of higher than 12 wt.%, ferritic, martensitic and duplex steels suffer from a serious aging embrittlement during the long-term aging at 300–500°C due to the phase separation of the α-(Fe, Cr) ferrite phase into Fe-rich ferrite (α) and the Cr-enriched ferrite (α') phases that can seriously degrade the mechanical properties [4-9]. This aging embrittlement is most severe, when the aging undergoes at 475°C, thus it is also called as "475°C embrittlement".

Besides Cr, Al is also an effective addition to enhance the corrosion and oxidation resistance of ODS steels at high temperatures [1, 10]. Recent findings by experiments [4,11,12] and simulation methods [13] suggest that Al can affect the 475°C embrittlement in Fe-Cr-Al alloys. However, the effect of Al on 475°C embrittlement in Fe-Cr-Al ferritic alloys is not thoroughly understood. It is also expected that the Zr and Hf, which are added in the Al-containing ODS steels to control the nanoparticle size [14], may alter the interaction between the oxide particle and the Cr-enriched α' phases and affect the age-hardening in ODS steels. Therefore, for optimizing the concentration and developing the reliable cladding of ODS steels, a systematic study of the effects of additions, such as Al, Cr and Zr, on the 475°C embrittlement in ODS steels is highly required.

* Corresponding author.
E-mail address: hanwentuo@hotmail.com (W. Han).

http://dx.doi.org/10.1016/j.nme.2016.05.015

Table 1
Chemical compositions of ODS ferritic steels and SUS430 steel (wt%).

Specimen		Chemical compositions (wt%)											Calculated value		
		C	Cr	W	Ti	Al	Y	Zr	O	N	Ar	Fe	Y_2O_3	ZrO_2	Ex.O
1	12Cr	0.027	11.78	1.9	0.23	<0.01	0.19	<0.01	0.13	0.006	0.006	Bal.	0.241	–	0.079
2	15Cr	0.028	14.12	1.83	0.22	<0.01	0.18	<0.01	0.12	0.007	0.006	Bal.	0.229	–	0.071
3	12Cr-5Al	0.029	11.72	<0.01	0.52	4.71	0.37	<0.01	0.23	0.006	0.006	Bal.	0.470	–	0.130
4	15Cr-5Al	0.031	14.16	<0.01	0.50	4.57	0.37	<0.01	0.22	0.005	0.006	Bal.	0.470	–	0.120
5	18Cr-5Al	0.034	16.78	<0.01	0.49	4.46	0.36	<0.01	0.22	0.004	0.006	Bal.	0.457	–	0.123
6	12Cr-7Al	0.028	11.86	<0.01	0.53	6.66	0.38	<0.01	0.22	0.005	0.006	Bal.	0.483	–	0.117
7	15Cr-7Al	0.031	14.18	<0.01	0.51	6.44	0.37	<0.01	0.22	0.006	0.006	Bal.	0.470	–	0.120
8	15Cr-7Al-0.4Zr-0.07Ex.O	0.033	14.66	<0.01	0.50	6.39	0.37	0.35	0.19	0.004	0.005	Bal.	0.470	0.47	0.090
9	15Cr-7Al-0.4Zr-0.014Ex.O	0.030	14.70	<0.01	0.50	6.38	0.36	0.36	0.25	0.005	0.005	Bal.	0.470	0.49	0.153
10	15Cr-7Al-0.4Zr-0.021Ex.O	0.029	14.76	<0.01	0.50	6.40	0.37	0.37	0.32	0.004	0.005	Bal.	0.470	0.50	0.220
11	18Cr-7Al	0.033	16.73	<0.01	0.49	6.28	0.37	<0.01	0.22	0.005	0.005	Bal.	0.470	–	0.120
12	12Cr-9Al	0.028	11.80	<0.01	0.53	8.60	0.37	<0.01	0.22	0.003	0.005	Bal.	0.470	–	0.120
13	15Cr-9Al	0.030	14.25	<0.01	0.51	8.40	0.37	<0.01	0.23	0.004	0.005	Bal.	0.470	–	0.130
14	18Cr-9Al	0.035	16.84	<0.01	0.50	8.16	0.37	<0.01	0.22	0.003	0.005	Bal.	0.470	–	0.120
15	SUS430	0.018	16.03	–	–	–	–	–	–	–	–	Bal.	–	–	–

In the present work, the age-hardening in 14 types of ODS ferritic steels with different concentrations of Cr, Al, and Zr were investigated. The effects of Cr, Al, and Zr additions on the hardness evolution during long-term aging at 475°C were evaluated and characterized.

2. Experimental procedure

Materials used in the present study were 14 different kinds of ODS ferritic steels with various Cr/Al contents. For investigating the effect of Zr on the age-hardening, a few of Zr-added 15Cr-7Al ODS steels were also fabricated. Detailed compositions of these ODSs are shown in Table. 1. The Ex. O in Table. 1 is the excess oxygen. The concentration of excess oxygen (Ex.O) was estimated as the total oxygen concentration minus the oxygen concentration in Y_2O_3. More details can be found in [15-16]. The powder mixing was achieved by mechanical alloying (MA) process, which was done with the ball-to-powder weight ratio of 15:1 and milling time of 48 hours by a high-energy attritor in an argon atmosphere. The resultant mixed powder was subsequently consolidated by hot extrusion at 1150°C, which had an area reduction ratio of 9.2. The diameter of the extruded rods was 25 mm.

Thermal aging was performed at 475 °C in a vacuum of 10^{-4} torr to prevent specimens form oxidation. Vickers hardness tests were carried out after several aging periods such as 135, 300, 700, 2000, and 5000 h. Hardness was tested 9 times at different positions for each individual specimen, and the average value was used to evaluate the hardness evolution. As a high test load (2 kg) was used during the hardness test, the indentations were measured as about 100 μm, and the hardness values are quite stable with deviations in the range of ± 5 HV. Microstructures were observed by transmission electron microscopy (TEM) with an accelerating voltage of 200 kV. The TEM specimens were prepared by twin-jet polishing with a solution composed of HClO4 and CH3COOH (1:19) at room temperature with a voltage of 20 V. Electron energy loss spectroscopy (EELS) technique was used to identify α' phases, since it is quite difficult to observe such a second phases, Cr-enriched α' phases, due to their small size and similar lattice constants with the matrix bcc Fe.

3. Results and discussion

Hardness evolutions of all these 14 types of ODS steels during the long-term aging up to 5000 h are summarized in Fig. 1. In the as-received condition, almost all the Al-added ODSs have lower hardness values than the Al-free ODSs. In authors' previous work [17, 18], it was found that Al addition resulted in coarsening the size, decreasing the number density and modifying the compositions and coherency of nanostructured oxide particles, which significantly affected the mechanical properties of ODS steels. In the non-aged ODSs with same Cr content, increasing Al addition from 5 to 9 wt.% causes increasing hardness, which is attributed to the solution strengthening of Al and/or the alteration of grain boundary structure induced during the thermo-mechanical process of fabrications.

The Zr effect in the non-aged ODS steels can also be found in Fig. 1 by comparing the Zr-added and Zr-free ODSs with same Cr/Al contents (15Cr-7Al). With Zr addtions, the 15Cr-7Al ODSs obviously show higher hardness values. The effect of Zr on microstructures of Al-added high-Cr ODS steels have been characterized in the previous report [14, 18] by comparing SOC-9 (Fe–15.5Cr–2W–0.1Ti–4Al–$0.35Y_2O_3$) and SOC-14 (Fe–15Cr–2W–0.1Ti–4Al–0.63Zr–$0.35Y_2O_3$).

During thermal aging, all these ODSs increase the hardness values, and achieve the maximal hardness values near 2000 h, indicating a saturation of age-hardening. In order to show the dependence of the hardening on the contents of Al and Cr, the amounts of hardening ($\Delta HV = HV_{aged} - HV_{non\text{-}aged}$) versus aging time are plotted for each content of Al and Cr in Fig. 2 and Fig. 3, respectively. The aging time dependence of ΔHV has the trend of three stages irrespective to steel compositions. At the early stage (0 h ~ 700 h), the hardness increases sharply, while in the second stage (700 h ~ 2000 h) ΔHV is saturated. After 2000 h aging, the hardness is rather stable and shows a trend of decreasing, suggesting that the α/α' phase separation has been done within 2000 h aging.

Besides the similarities in the age-hardening behavior among these alloys, different characteristics can also be seen according to the effect of Cr/Al contents, as shown in Fig. 2. Particularly, the 18Cr-ODSs with 5Al and 7Al exhibit the most remarkable increase of hardness, with ΔHV values of 87.9 HV and 81.2 HV, respectively. These phenomena strongly indicate that the 18Cr-5Al- and 18Cr-7Al-ODSs undergone an exclusive mechanism of hardness increase.

A typical example of TEM observation of α'-phase is shown in Fig. 4 for 18Cr-5Al-ODS aged for 5000 h. The Cr-enriched α'-phase, which has a mean diameter of about 9 nm and a high number density, is effectively detected and presented in the EELS map of Cr (Fig. 4b). It verifies that the α/α' phase separation significantly occurred during the long-term aging process at 475°C. Because of the generation of the Cr-enriched α' phase, 18Cr-5Al-ODS shows the most significant hardening tendency. In addition, the 18Cr-5Al also shows a much higher increasing rate than the 15Cr- and 12Cr-5Al ODSs. Even aged 300 h, the ΔHV of 18Cr-5Al is more than

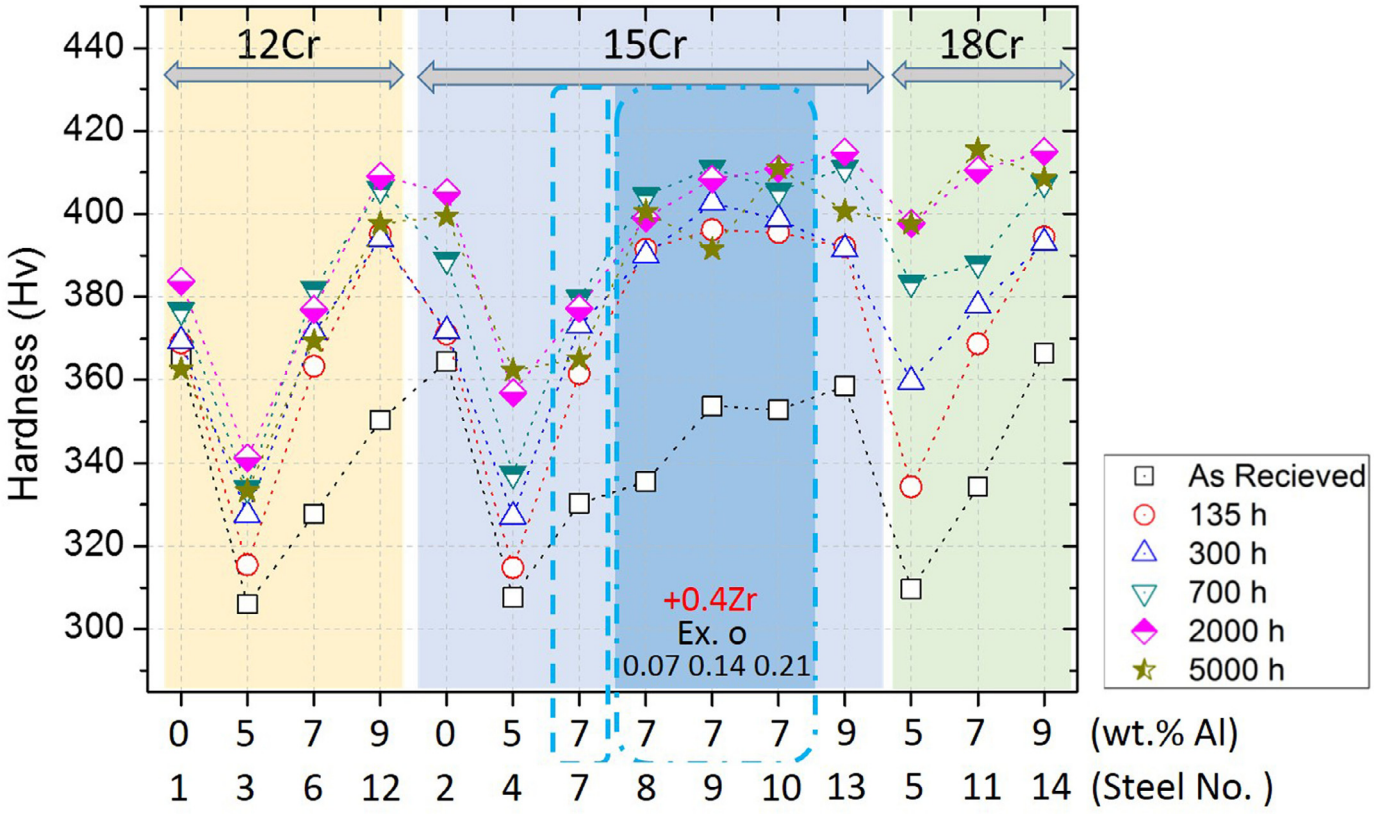

Fig. 1. Hardness evolution of the ODS steels with different contents of Cr/Al during thermal aging at 475°C till 5000 h.

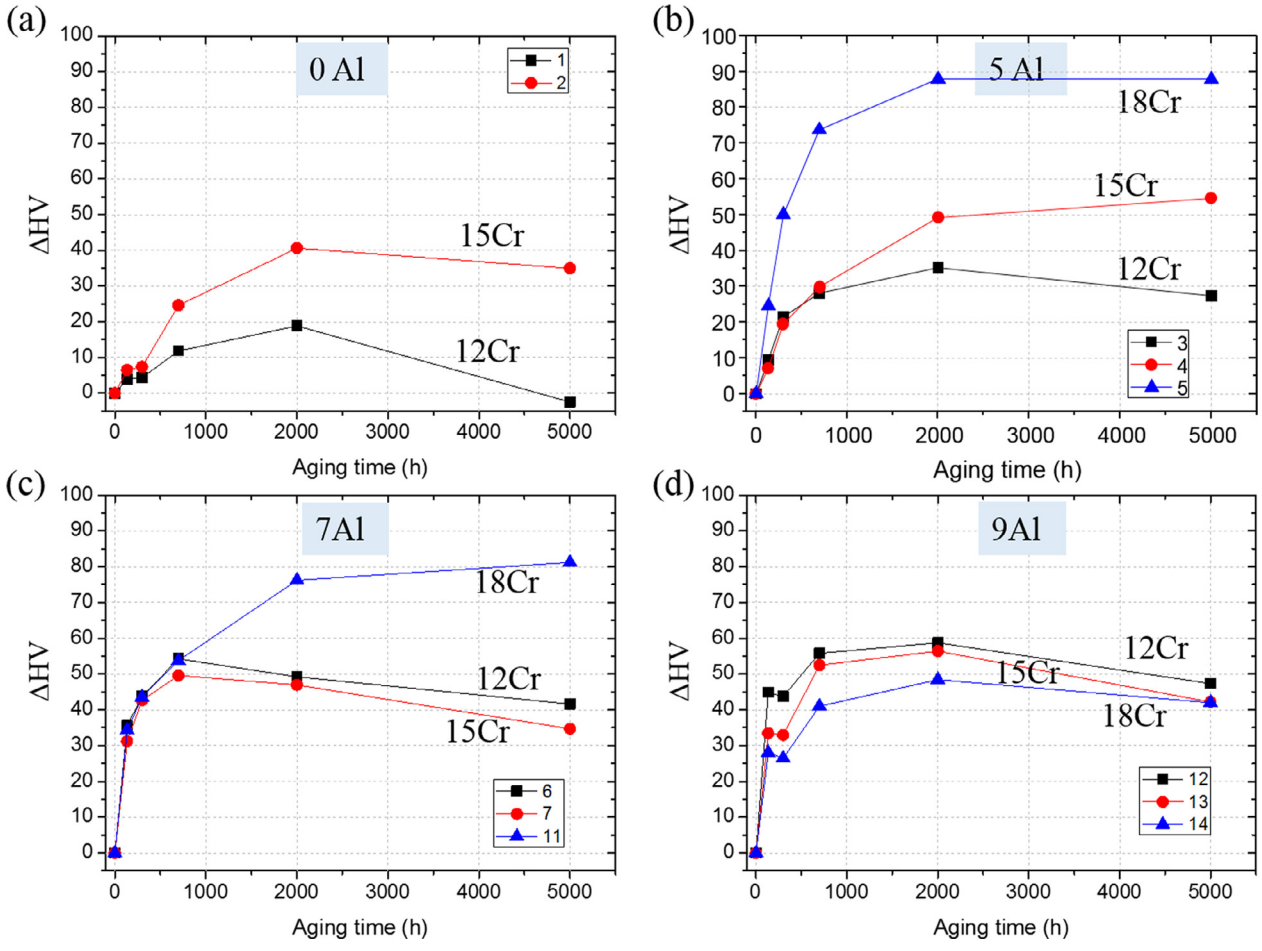

Fig. 2. The plots to show the effect of Cr on ΔHV in the steel groups with same Al content.

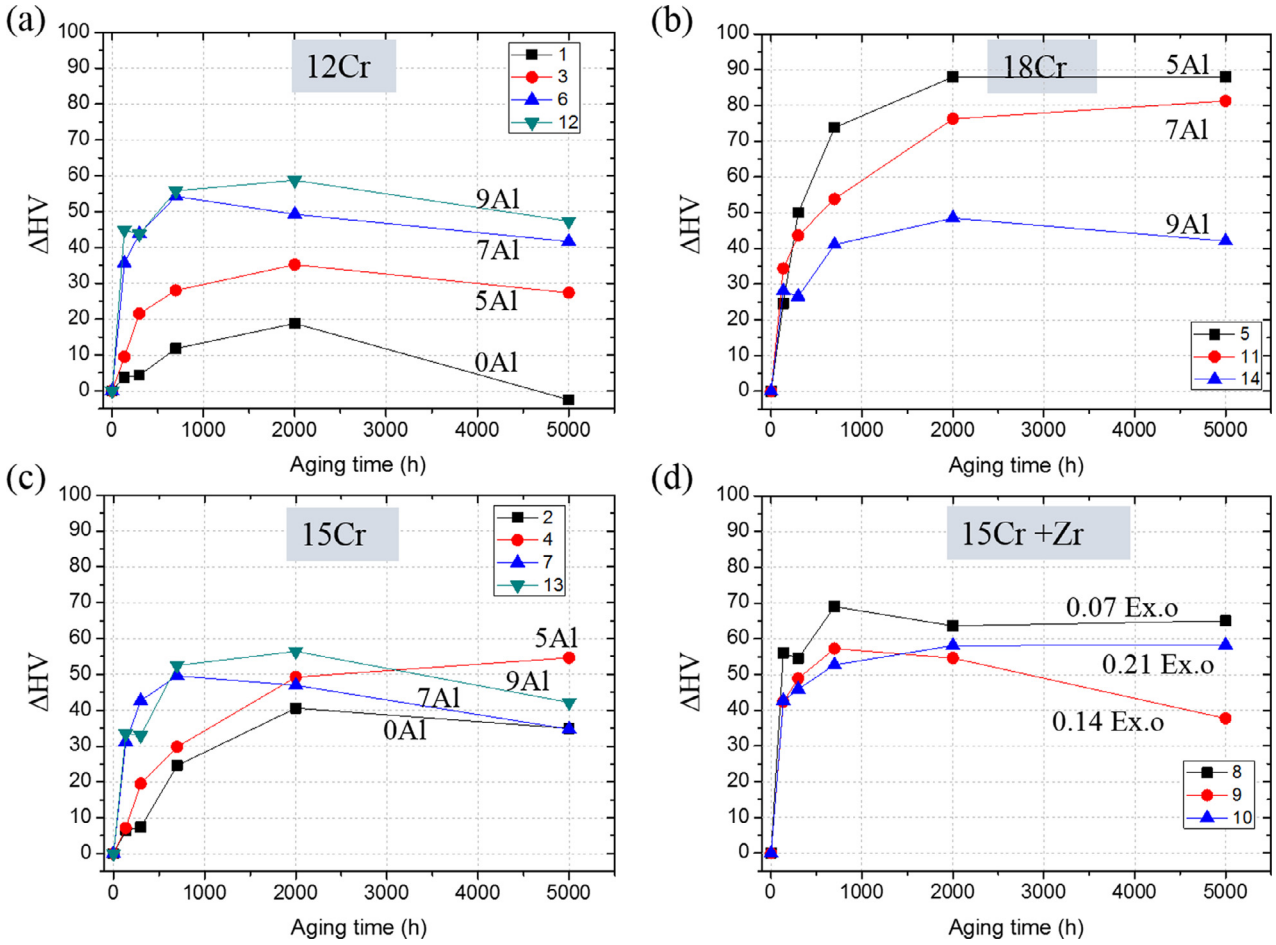

Fig. 3. The plots to show the effect of Al on ΔHV in the steel groups with same Cr content.

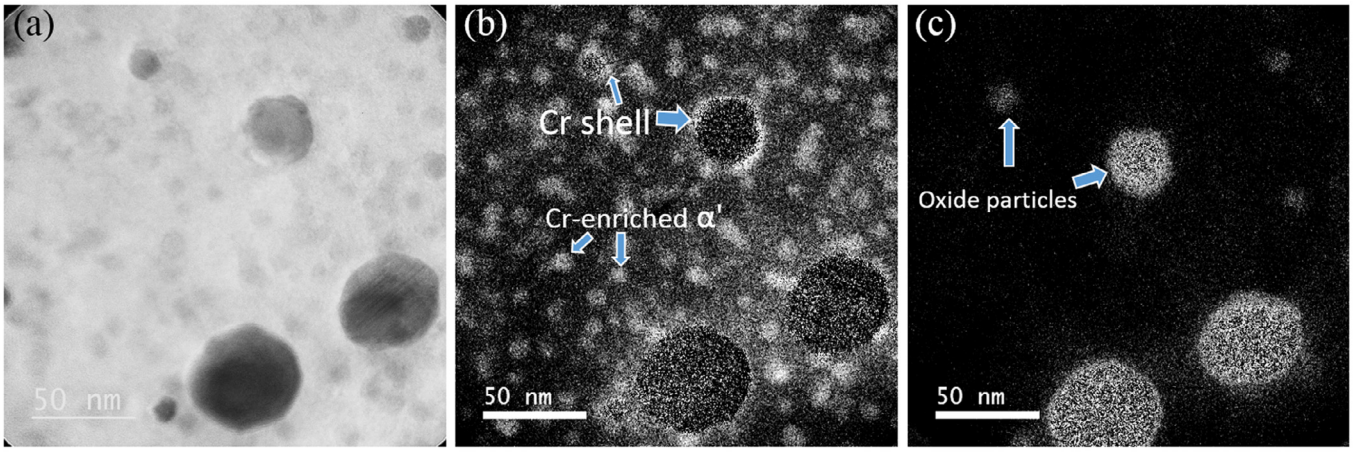

Fig. 4. TEM observations of 18Cr-5Al ODS steel after aging at 475°C for 5000h: (a) bright field image; (b) ELLS map of Cr; (c) ELLS map of O.

50Hv. Similar results are also observed in PM 2000 ODS steel (Fe–18.6 wt.% Cr–5.2% Al) [11,12]. Capdevila [12] reported that the α/α' phase separation can occur only after ageing for 100 h in the PM 2000 ODS steels on the bases of observations by atom probe tomography. The quick α/α' phase separation process contributes to the early hardening in 18Cr-5Al ODS steels. The early hardening in 12Cr-ODS steels with high Al content needs more detailed analysis of microstructure.

The α/α' phase separation depends on material compositions. Kobayashi [4] illuminated this aspect by using a diffusion multiple technique in ferritic ternary alloys with a wide composition range of Fe–(10–30)Cr–(0–20)Al (at.%) during aging at 475°C. Based on the data obtained in this research, a draft triangular diagram is mapped as Fig. 5, where 18Cr-5Al is obviously located in the α' region, which coincides well with our TEM observations mentioned above. The map also suggests the phase separation should not occur in the composition of 18Cr-7Al. However, hardness results of

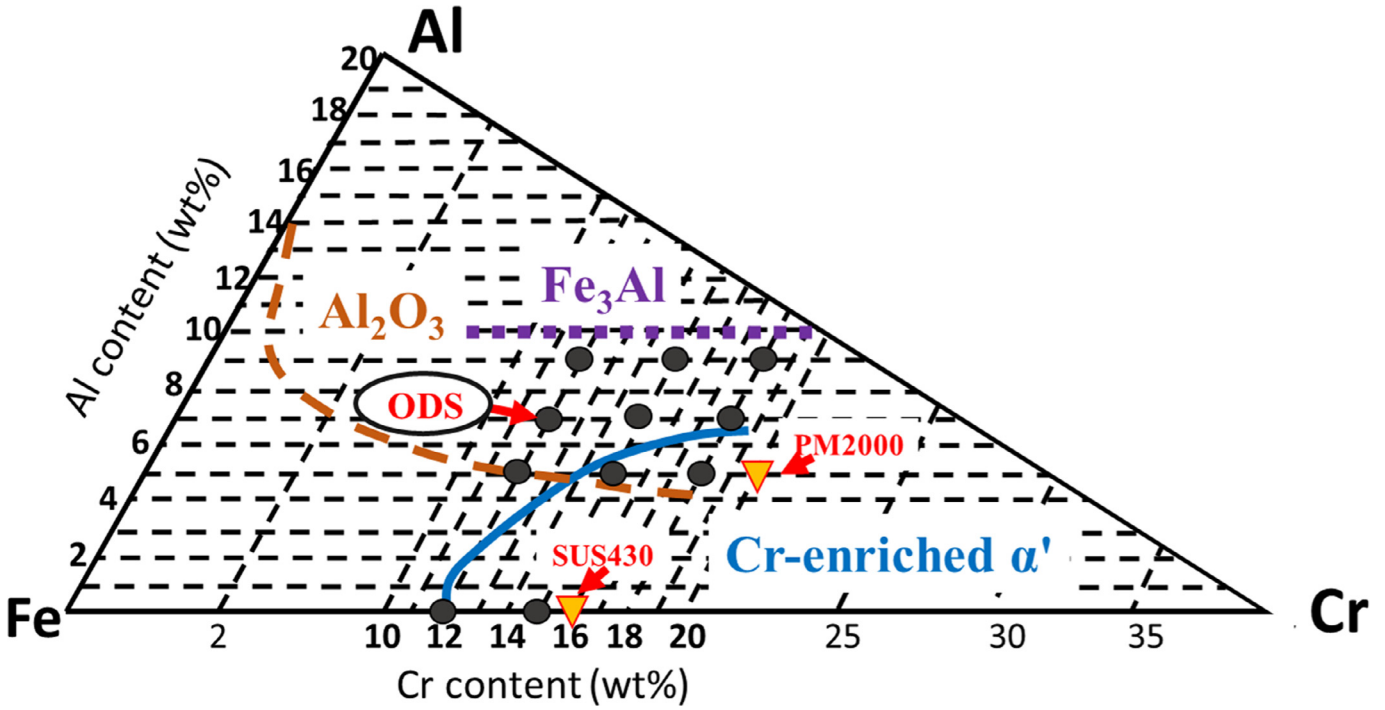

Fig. 5. Fe-Cr-Al ternary diagram: Black spots and triangles represent compositions of ODS steels investigated in the presented work and the commercial steels, respectively; The Al_2O_3 formation zone at 1100°C is bounded by a broken line; The zones of Fe3Al and Cr-enriched α' phase at 475°C are bounded by a dotted line and a solid line, respectively.

18Cr-7Al (as shown in Fig. 2c and Fig. 3b) shows a similar ΔHV level with 18Cr-5Al, that strongly indicates Cr-enriched α' phase is generated in 18Cr-7Al ODS alloy during aging. The differences between the presented results and the ref. [4] can be interpreted as follows: first of all, the compositions of the presented ODS steels are much complicated than that of the Fe-Cr-Al ternary model alloy in ref. [4]. Besides Al, other additions, such as Ti, Y and Zr may also interact with Cr, and may affect the formation and/or interface energies of the Cr-enriched α' phase during the phase separation. In addition, the ODS steels have complicated microstructures, which include a number of oxide particles and fine elongated grains that may alter the elemental process of the diffusion of Cr atoms and the nucleation of the α' phase. Therefore, more microstructural observations of wide variety of ODS steels with different compositions and aging times are necessary to draw out the precise phase separation diagram of Cr-Al-ODS steels.

Concerning the Al dependence, the 12Cr-ODSs (Fig. 3a) obviously shows the increase ofΔHV with higher Al addition. However, this tendency is opposite in the 18Cr-ODSs. In Fig. 3b, the 18Cr-5Al shows the highest ΔHV, while the ΔHV of 18Cr-9Al is quite limited and has the similar level with the 12Cr-9Al (Fig. 2d). Our TEM observation of the 18Cr-9Al evidences that no α' phase has been generated after 5000 h aging. It clearly verifies that 9Al can suppress the phase separation and the generation of Cr-enriched α' phases in 18Cr-ODS during aging, and shift the boundary of the $\alpha+\alpha$' two phase region toward much higher Cr content. The reason can be attributed to the modification of the interfacial energy and formation energies during the phase separation by adding Al. Based on the first-principles simulation [13], the suppression of the formation and retardation the coarseness of the α' phase by adding Al is due to the thermo-dynamical reasons that Al can affect the interfacial energy in the preliminary stage during the phase separation and the formation energies in the later stage.

Although these 14 types of ODS steels show different susceptibility to the age-hardening, the hardening tendency of ODS steels is still much lower than non-ODS steels with high-Cr additions. This characteristic can be found in Fig. 6 by comparing the evolution of ΔHV between 15Cr-0Al ODS and SUS430 steels. The SUS430 steel, which is a non-ODS steel with 16 wt.% Cr, shows a drastic age-hardening with a ΔHV value of 100 HV after 5000 h aging, which is more than twice of the ΔHV in 15Cr-0Al ODS steel. The low susceptibility to age-hardening of ODS steels may be attributed to the nanostructured oxide particles. The EELS Cr map (Fig. 4b) visibly shows that the oxide particles are surrounded by the Cr-enriched shell. It indicates oxide particles could affect the diffusion path of Cr, retard the formation of the individual Cr-enriched α' phase, and thus affect the age-hardening. The distribution morphology of oxide particles may also affect the age-hardening. One evidence can be found by comparing the Zr-added (Fig. 3d) with Zr-free (Fig. 3c) 15Cr-7Al ODS steels. As the minor element Zr is added, the ODS steels in Fig. 3d appears to show a higher age-hardening than the Zr-free 15Cr-7Al ODS steel.

4. Conclusions

The age-hardening in oxide dispersion strengthened (ODS) ferritic steels with various additions of Cr (12, 15 and 18 wt.%) and Al (0, 5, 7 and 9 wt.%) were investigated.

In low Al (0Al and 5Al) ODS steels, increasing Cr concentration resulted in increasing the amout of age-hardening, while almost no Cr dependence can be found in the 9Al ODS steels. The 12Cr-ODS steels show an obvious Al dependence that the age-hardening is enhanced with increasing the Al content. However, the 18Cr-ODS steels show an opposite tendency to the 12Cr-ODS steels: increasing Al addition suppresses the age-hardening. The TEM observations reveal that no α' phase is formed in the 18Cr-9Al-ODS steel, while a number of Cr-enriched α' phases can be generated in the 18Cr-5Al steel. The Zr addition enhances the age-hardening, and the amout of the hardening is also affected by the Ex. O. Although all the tested ODS steels show the age-hardening during the long-term aging at 475°C, the age-hardening susceptibility of ODS steels

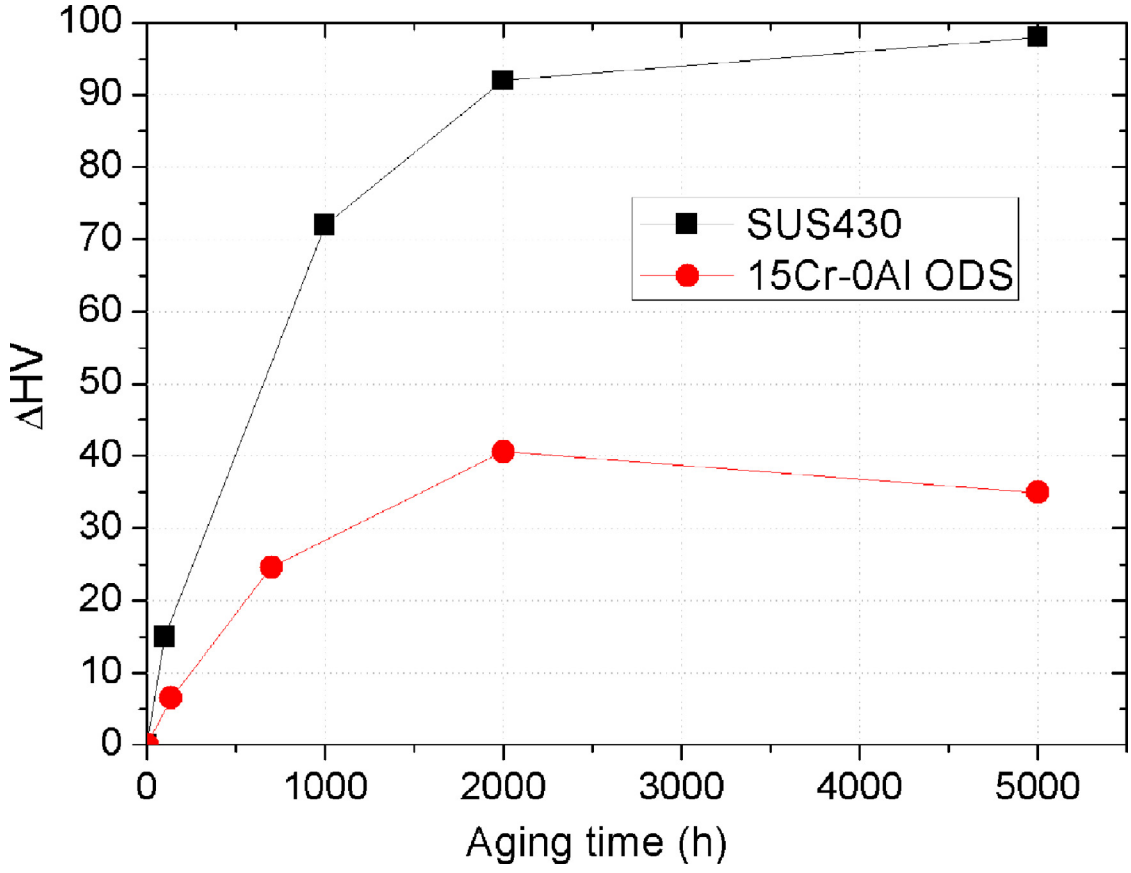

Fig. 6. Comparison of ΔHV between 15Cr-0Al ODS and SUS430 steels.

is much lower than the non-ODS steel with the similar Cr concentration.

Acknowledgement

The present study includes the result of "Accident tolerant ODS steels R&D" entrusted to "Hokkaido University" by the Ministry of Education, Culture, Sports, Science and Technology of Japan (MEXT).

References

[1] A. Kimura, R. Kasada, N. Iwata, H. Kishimoto, C. Zhang, J. Isselin, P. Dou, J. Lee, N. Muthukumar, T. Okuda, J. Nucl. Mater. 417 (2011) 176–179.
[2] W. Han, D. Chen, Y. Ha, A. Kimura, H. Serizawa, H. Fujii, Y. Morisada, Scripta Mater. 105 (2015) 2–5.
[3] S. Ukai, T. Nishida, H. Okada, T. Okuda, M. Fujiwara, K. Asabe, J. Nucl. Sci. Technol. 34 (1997) 256–263.
[4] S. Kobayashi, T. Takasugi, Scripta Mater. 63 (2010) 1104–1107.
[5] J.K. Sahu, U. Krupp, R.N. Ghosh, H.J. Christ, Mater. Sci. Eng. A 508 (2009) 1–14.
[6] P. Grobner, Metall. Trans. 4 (1973) 251–260.
[7] M. Miller, J. Hyde, M. Hetherington, A. Cerezo, G. Smith, C. Elliott, Acta Metall. Mater. 43 (1995) 3385–3401.
[8] D. Chen, A. Kimura, W. Han, J. Nucl. Mater. 455 (2014) 436–439.
[9] D. Chen, A. Kimura, C. Zhang, W. Han, in: PRICM: 8 Pacific Rim International Congress on Advanced Materials and Processing. Wiley Online Library, pp. 529–535.
[10] T. Liu, C. Wang, H. Shen, W. Chou, N.Y. Iwata, A. Kimura, Corros. Sci. 76 (2013) 310–316.
[11] C. Capdevila, M.K. Miller, K.F. Russell, J. Mater. Sci. 43 (2008) 3889–3893.
[12] C. Capdevila, M.K. Miller, K.F. Russell, J. Chao, J.L. González-Carrasco, Mater. Sci. Eng. A 490 (2008) 277–288.
[13] W. Li, S. Lu, Q.-M. Hu, H. Mao, B. Johansson, L. Vitos, Comp. Mater. Sci 74 (2013) 101–106.
[14] P. Dou, A. Kimura, R. Kasada, T. Okuda, M. Inoue, S. Ukai, S. Ohnuki, T. Fujisawa, F. Abe, J. Nucl. Mater 444 (2014) 441–453.
[15] S. Ukai, T. Kaito, S. Otsuka, T. Narita, M. Fujiwara, T. Kobayashi, ISIJ Int. 43 (12) (2003) 2038–2045.
[16] T.k. Kim, C.S. Bae, D.H. Kim, J. Jiang, S.H. Kim, C.B. Lee, D. Hahn, Nucl. Eng. Technol 40 (4) (2008) 305–310.
[17] P. Dou, A. Kimura, T. Okuda, M. Inoue, S. Ukai, S. Ohnuki, T. Fujisawa, F. Abe, Acta Mater 59 (3) (2011) 992–1002.
[18] A. Kimura, N. Iwata, H. Kishimoto, C.H. Zhang, in: Proceeding 2009 International Congress Advances in Nuclear Power Plants (ICAPP 09), Tokyo, Japan, 9920, 2009, pp. 9921–9928.